

Supplementary Material for “Direct photolysis of carbonyl compounds dissolved in cloud and fog droplets”

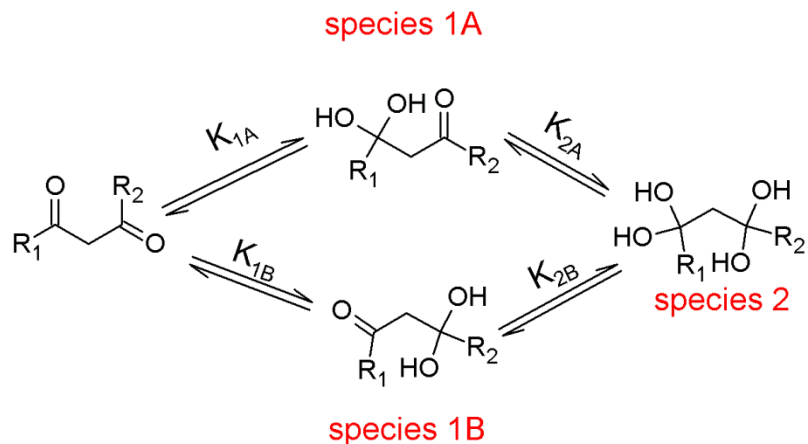
*Scott A. Epstein, Enrico Tapavicza, Filipp Furche, and Sergey A. Nizkorodov**

Department of Chemistry, University of California, Irvine,

1102 Natural Sciences 2, Irvine, CA 92697-2025

Hydration of Dicarboxyls

This section describes our approach to account for hydration equilibria in dicarbonyl compounds. Consider an unhydrated and unsymmetrical dicarbonyl with carbonyl groups identified by the letters “A” and “B” (Scheme S1). In the aqueous phase, hydration can reversibly replace carbonyl “A” with a gem-diol group forming species 1A (equilibrium constant for the hydration process, $K_{\text{hyd}} = K_{1A}$) and/or carbonyl “B” with a gem-diol group forming species 1B ($K_{\text{hyd}} = K_{1B}$). A certain fraction of the mixture may be double hydrated, with both carbonyl groups converted in the gem-diol form. The corresponding equilibrium constants, K_{2A} and K_{2B} are identified in scheme S1.



Scheme S1: Hydration of a generic dicarbonyl

The molar fraction that is unhydrated, α_{un} , fully-hydrated, α_{fh} , and partially-hydrated, α_{ph} , can be derived from the equilibrium equations (all activity coefficients are set to unity):

$$\alpha_{uh} = (1 + K_{1A} + K_{1B} + K_{1B}K_{2B})^{-1} \quad (1)$$

$$\alpha_{fh} = ((K_{1B}K_{2B})^{-1} + K_{2A}^{-1} + K_{2B}^{-1} + 1)^{-1} \quad (2)$$

$$\alpha_{ph} = 1 - (\alpha_{uh} + \alpha_{fh}) \quad (3)$$

Because the gem-diol form is lacking the $\pi^* \leftarrow n$ transition associated with the carbonyl group, it is appropriate to assume that the rates of photolysis of the singly hydrated dicarbonyl species are approximately one-half of the rate of photolysis of the unhydrated form, resulting in the following expression for Z:

$$Z = \frac{\frac{dn_{hv}^{gas}}{dt}}{\frac{dn_{hv}^{aq}}{dt}} \geq \frac{\alpha_{uh} + 0.5\alpha_{ph}}{(R \cdot T \cdot LWC_v \cdot k_H)} \quad (4)$$

This assumption will not hold for compounds that carry carbonyl groups on the adjacent carbon atoms and for carbonyl groups that are part of a conjugated system.

Extinction Coefficients of Aqueous D-Glyceraldehyde and Dihydroxyacetone

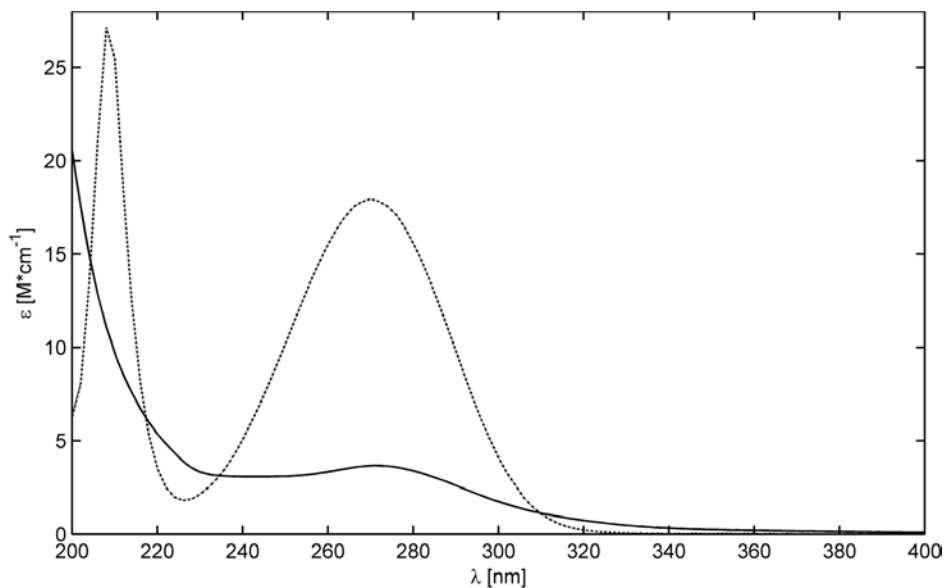


Figure S1: Molar extinction coefficients for D-glyceraldehyde (solid curve) and dihydroxyacetone (dashed curve) at 25°C.

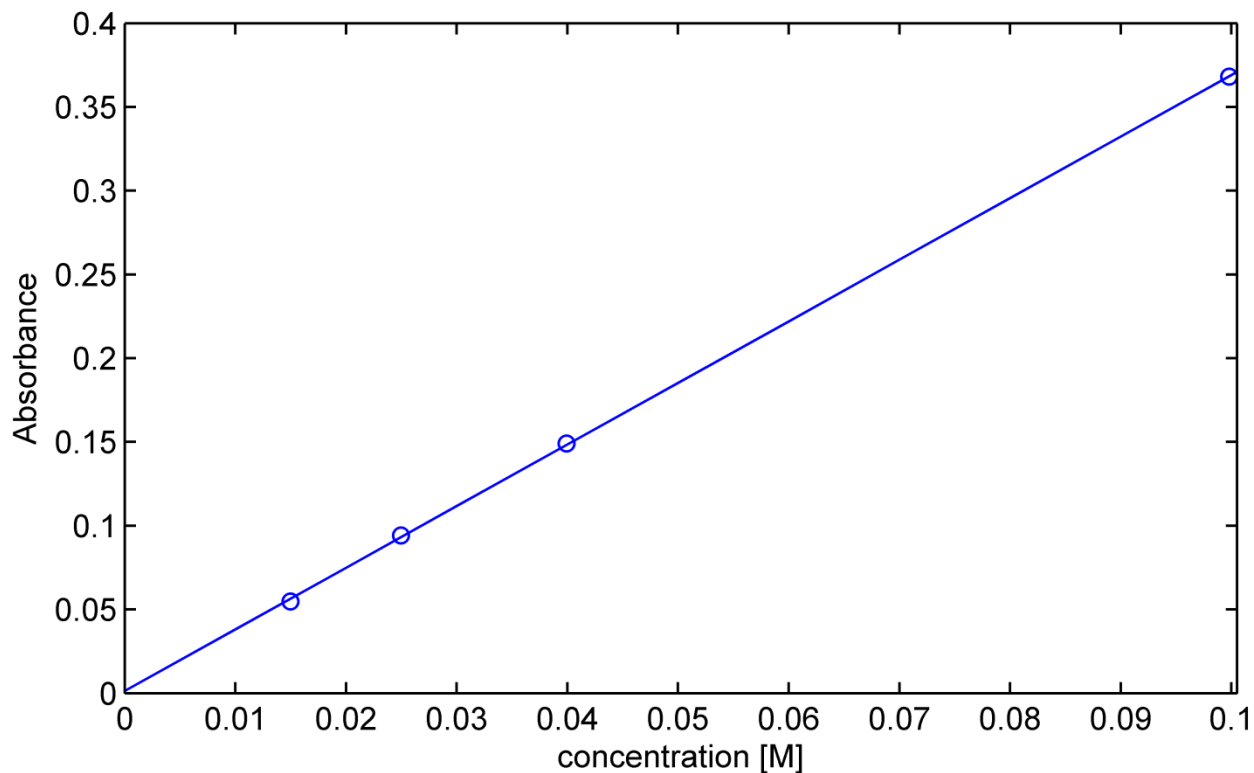


Figure S2: D-glyceraldehyde absorbance as a function of concentration of the free form

Figure S1 shows the molar extinction coefficients for D-glyceraldehyde (solid curve) and dihydroxyacetone (dashed curve) at 25°C that were measured in this work. A Beer-Lambert plot of the measurements is shown in Figure S2. Tabulated extinction coefficients are attached in a Microsoft Excel supporting information file. Both glyceraldehyde and dihydroxyacetone exhibit

a well defined $\pi^* \leftarrow n$ band that overlaps the solar flux. The $\pi^* \leftarrow n$ band in D-glyceraldehyde is considerably lower in intensity compared to that in dihydroxyacetone because the former is much more prone to hydration than the latter. Specifically, the observed extinction coefficient is reduced relative to the extinction coefficient of the unhydrated form of the molecule:

$$\epsilon_{observed} = \frac{\epsilon_{unhydrated}}{1 + K_{hyd}} \quad (5)$$

For D-glyceraldehyde, this reduction is substantial as $1 + K_{hyd} = 18.3$ (Glushonok et al., 1986), much smaller than the corresponding value for dihydroxyacetone, $1 + K_{hyd} = 1.77$ (Glushonok et al., 2003; Davis, 1973).

FTIR Spectrum of Gaseous Photolysis Products

Photolysis of aqueous D-Glyceraldehyde produced gas bubbles that formed on the walls of the photolysis cell. The gases produced during photolysis of aqueous D-Glyceraldehyde at 25°C were captured and analyzed with a Fourier Transform Infrared (FTIR) spectrometer (Mattson Galaxy Series 5000). A diagram illustrating the FTIR cell is presented in Figure S3.

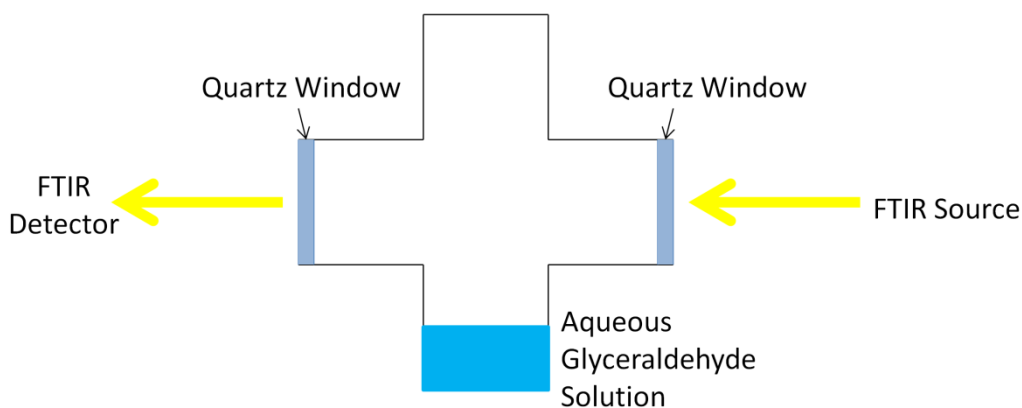


Figure S3: Apparatus used to capture and analyze the gases evolved from photolysis of glyceraldehyde

The FTIR spectrum shown in Figure S4 indicates the presence of carbon monoxide. Carbon monoxide is an expected product of the direct photolysis of D-Glyceraldehyde. We have not attempted to quantify the yields of this product. The FTIR spectrum also indicates the presence of carbon dioxide, a potential product of secondary photolysis. However, we cannot conclude that the carbon dioxide evolved from the photolysis due to the potential presence of CO₂ from the ambient air.

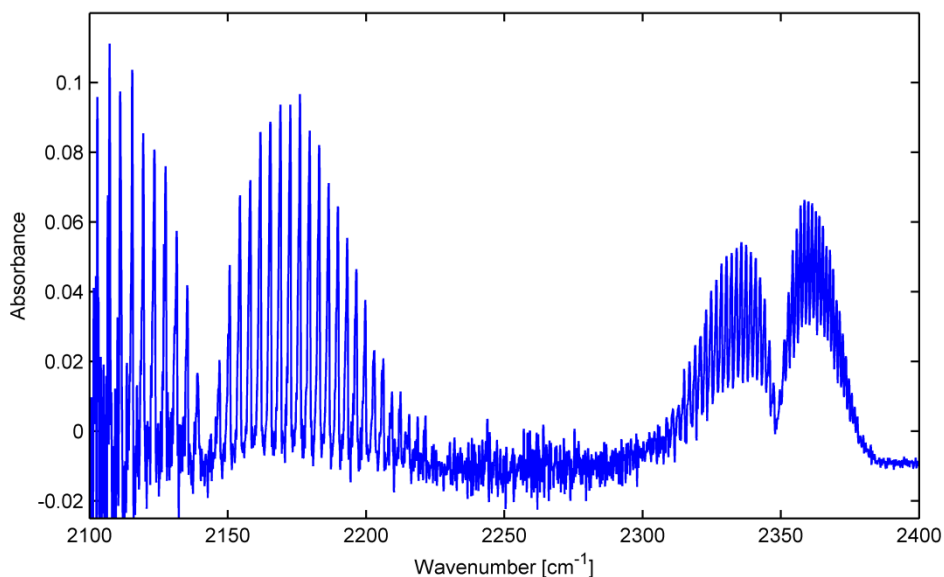


Figure S4: FTIR spectrum of the products of aqueous D-glyceraldehyde photolysis at 25°C. The band centered at 2143 cm^{-1} belongs to carbon monoxide, and the band centered at 2349 cm^{-1} is the asymmetric stretch of CO_2 .

Monitoring the Photolysis of Glyceraldehyde Using a UV-Vis Spectrometer

We took UV-Vis spectra measurements during photolysis of 0.1 M aqueous glyceraldehyde solutions at various photolysis times. Figure S5 shows how the absorption of an aqueous glyceraldehyde solution changes when exposed to UV light at 25°C.

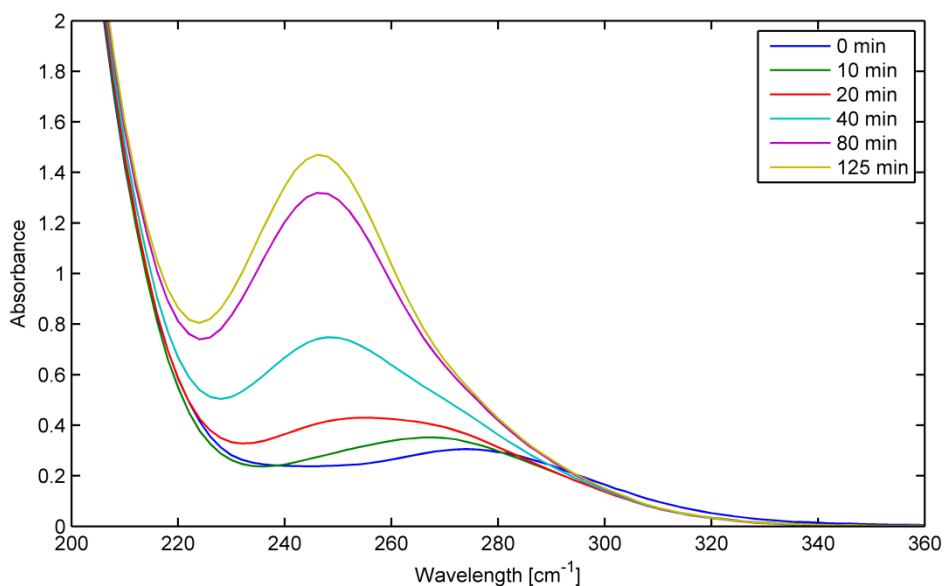


Figure S5: Absorption of glyceraldehyde photolysis solution as a function of time at 25°C

Upon photolysis, the $\pi^* \leftarrow n$ band undergoes a simultaneous hypsochromic and hypochromic shift. We believe that the band growing at 250 nm belongs to a minor but strongly absorbing photolysis product (which we could not identify).

Monitoring the Photolysis of D-Glyceraldehyde with ESI-MS

We calibrated the ESI-MS technique for determining glyceraldehyde solution concentration before each photolysis experiment. Several glyceraldehyde solutions of varying concentrations were derivatized with Girard Reagent T (GT) and analyzed with an ESI-MS. Tetraethylammonium chloride was added to the GT solution to act as an internal standard. Figure S6 illustrates a typical calibration curve determined with this method. The calibration is approximately linear.

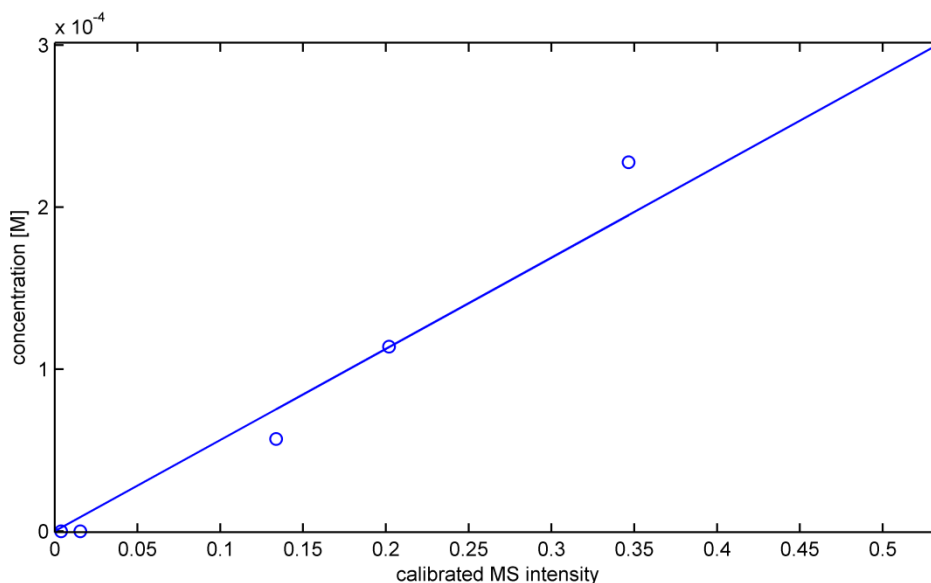


Figure S6: Results of a calibration experiment relating the concentration of glyceraldehyde and the peak intensity of the derivatized glyceraldehyde adduct. The calibrated mass spec (MS) intensity is the response of the glyceraldehyde-GT complex scaled by the response of tetraethylammonium chloride.

During a photolysis experiment, small aliquots of the glyceraldehyde solution were diluted with the GT/tetraethylammonium chloride solution and allowed to react overnight, forming the GT-glyceraldehyde adduct. The MS intensity—the response of the glyceraldehyde-GT complex scaled by the response of tetraethylammonium chloride—was scaled by the initial MS intensity and plotted in Figure S7.

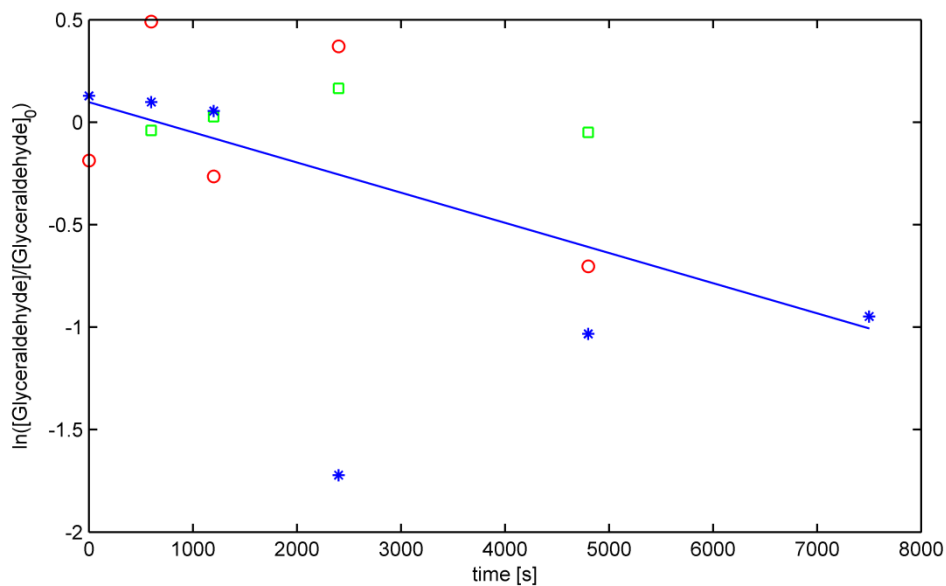


Figure S7: Semi-quantitative measurements of glycerinaldehyde concentration as a function of photolysis time at 25°C for three separate experiments.

The observed scatter is due to the difficulties in quantifying the derivatized product with ESI-MS. The experiment indicated with the blue asterisks has an extreme outlier at 2300 s. However this outlier does not significantly affect the slope of the fitted line as it is close to the center of the x-axis. The slope of the fitted line, along with the known flux from the UV lamp obtained from actinometer measurements, were used to approximate the quantum yield of photolysis.

ESI-MS measurements were also used to identify potential photolysis products. Figure S8 shows an ESI-MS difference spectrum. Positive peak heights indicate that a product was formed while negative peak heights indicate the consumption of a reactant.

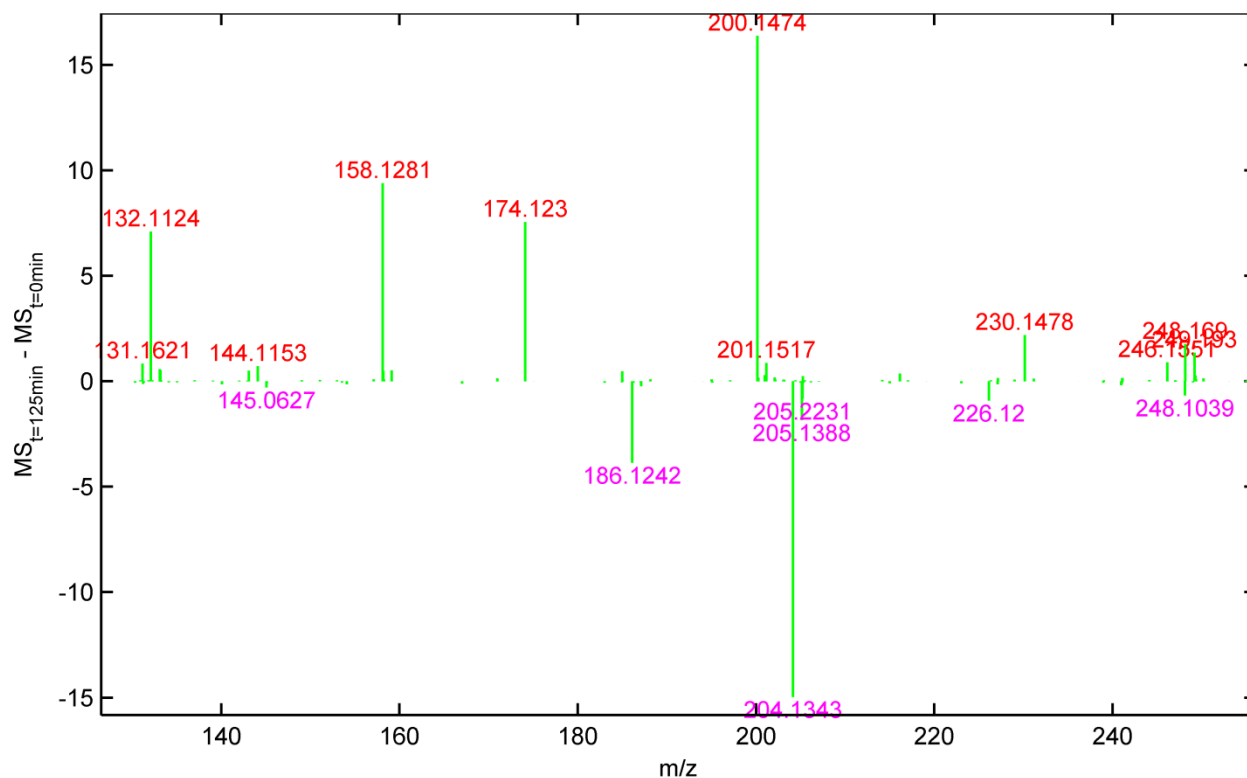


Figure S8: ESI-MS difference spectrum showing the formation of products and the disappearance of reactants from a typical glycerinaldehyde photolysis experiment

Peak m/z was calibrated with a two point calibration using tetraethylammonium chloride (exact mass $130.1590 \text{ g mol}^{-1}$) and the glycerinaldehyde+GT adduct ($204.1343 \text{ g mol}^{-1}$). Free GT molecules dissociated from Cl^- appear at 132.1124 (exact mass $132.1131 \text{ g mol}^{-1}$). The product appearing at 158.1281 is likely the ethanal+GT adduct ($158.1392 \text{ g mol}^{-1}$) while the product appearing at 174.123 is likely the glycolaldehyde+GT adduct ($174.1269 \text{ g mol}^{-1}$). No other possible products appear in each mass range after considering the resolution of the instrument. To further confirm the presence of these products, we spiked several solutions with both ethanal and glycolaldehyde. A single peak for each adduct remained. Several other contaminants were consumed and products were formed. However, we were unable to unambiguously assign molecules to these species.

Reproductions of Figure 6 Under Different Atmospheric Conditions

To test how atmospheric conditions affect the identification of products that may have significant aqueous photolysis rates, two reproductions of figure 6 under varying atmospheric conditions are presented in Figures S9 and S10. Figure S9 illustrates how solar zenith angle affects the significance of aqueous photolysis.

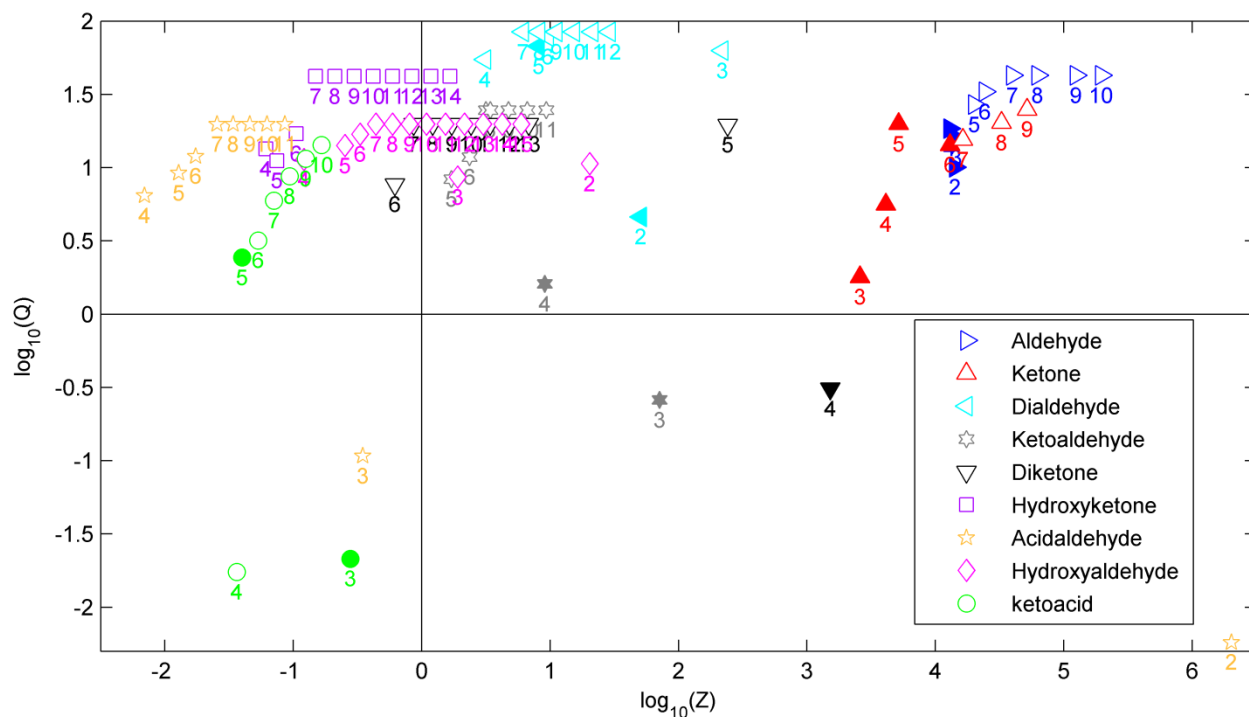


Figure S9: Reproduction of Figure 6 in manuscript with a solar zenith angle of zero degrees. Aqueous hydroxyl radical concentration is 10^{-13} M, $T = 25^{\circ}\text{C}$, and $\text{LWC} = 0.5 \text{ g m}^{-3}$.

Decreasing the solar zenith angle to its maximum value of zero degrees slightly decreases the Q value for every compound because the maximum rate of aqueous photolysis increases due to increased overlap between the actinic flux and the molar extinction coefficient. However, this decrease in SZA does not affect the conclusions of our analysis. Aqueous photolysis may be important for only three of the compounds studied in the plot: pyruvic acid, 3-oxobutanoic acid, and 3-oxopropanoic acid. The effects of decreasing the aqueous hydroxyl radical concentration to a level more commonly seen at night are illustrated in Figure S10.

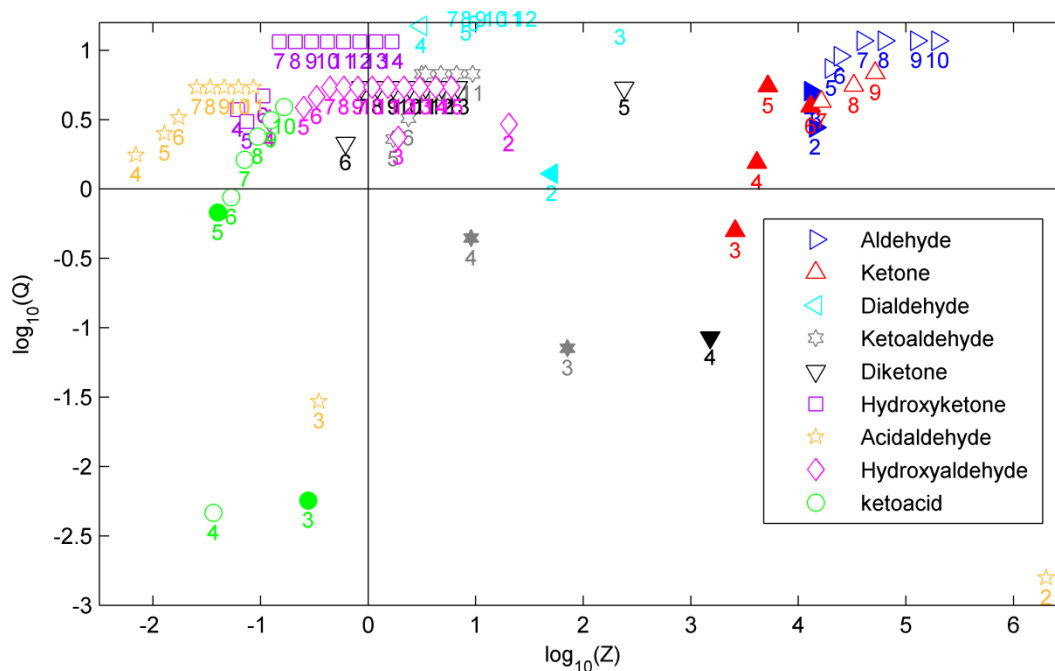


Figure S10: Reproduction of Figure 6 in the manuscript with an aqueous hydroxyl radical concentration of 10^{-14} M. Solar zenith angle is 20° , $T = 25^\circ\text{C}$, and $\text{LWC} = 0.5 \text{ g m}^{-3}$.

As in Figure S9, decreasing the aqueous OH concentration decreases the value of Q for all compounds. Two additional compounds enter the region where aqueous photolysis may be significant: 3-oxopentanoic acid and 3-oxohexanoic acid. However, situations where aqueous OH concentrations are 10^{-14} M with sunlight at a SZA of 20° are likely uncommon. The literature values used to generate these plots are presented below.

Literature Values for ϵ_{max} and λ_{max}

Table S1: ϵ_{max} and λ_{max} values used to generate Figures 6, S9, and S10. The upper row indicates the number of carbons in a molecule with a functionality specified by the first column. Bold values were obtained from the literature with the corresponding references in Table S2. For compounds without published data, an upper estimate was used based on the properties of molecules with similar functionalities.

		2	3	4	5	6	7	8	9	10	11	12	13	14	15
Aldehyde	ϵ_{max}	8.1	13.1	13.5	15	15	15	15	15	15	15	15	15	15	15
	λ_{max}	277.5	277.5	282.5	282.5	282.5	282.5	282.5	282.5	282.5	282.5	282.5	282.5	282.5	282.5
Ketone	ϵ_{max}		17.6	17.9	24	21.2	25	25	25	25	25	25	25	25	25
	λ_{max}		270	277.5	271	279	280	280	280	280	280	280	280	280	280
Dialdehyde	ϵ_{max}	5.8	8	8	7.9	8	8	8	8	8	8	8	8	8	8
	λ_{max}	267.5	282	282	282	282	282	282	282	282	282	282	282	282	282

Keto-aldehyde	ϵ_{\max}		16	13	20	20	20	20	20	20	20	20	20	20	20
	λ_{\max}		284	280	285	285	285	285	285	285	285	285	285	285	285
Diketone	ϵ_{\max}			26.5	25	25	25	25	25	25	25	25	25	25	25
	λ_{\max}			284	285	264	285	285	285	285	285	285	285	285	285
Hydroxy-ketone	ϵ_{\max}		20	20	20	20	20	20	20	20	20	20	20	20	20
	λ_{\max}		267	270.5	280	280	280	280	280	280	280	280	280	280	280
Acid-aldehyde	ϵ_{\max}	25	25	25	25	25	25	25	25	25	25	25	25	25	25
	λ_{\max}	285	285	285	285	285	285	285	285	285	285	285	285	285	285
Hydroxy-aldehyde	ϵ_{\max}	25	25	25	25	25	25	25	25	25	25	25	25	25	25
	λ_{\max}	277	285	285	285	285	285	285	285	285	285	285	285	285	285
Ketoacid	ϵ_{\max}		19.5	25	25.1	25	25	25	25	25	25	25	25	25	25
	λ_{\max}		317.5	317.5	270	285	285	285	285	285	285	285	285	285	285

Table S2: References for ϵ_{\max} and λ_{\max} values used to generate Figures 6, S9, and S10. The upper row indicates the number of carbons in a molecule with a functionality specified in the first column. “E” indicates that an upper estimate was used. Ref 1 (Mackinney and Temmer, 1948); Ref 2 (Xu et al., 1993); Ref 3 (Rice, 1920); Ref 4 (Malik and Joens, 2000); Ref 5 (Schutze and Herrmann, 2004); Ref 6 (Martinez et al., 1975); Ref 7(Gubina et al., 2004); Ref 8 (Steenken et al., 1975); Ref 9 (Maroni, 1957); Ref 10 (Beeby et al., 1987)

	1	2	3	4	5	6	7	8	9	10	11	12	13	14	15
Aldehyde	ϵ_{\max}	1	1	1	E	E	E	E	E	E	E	E	E	E	E
	λ_{\max}	1	1	1	E	E	E	E	E	E	E	E	E	E	E
Ketone	ϵ_{\max}		2	2	2	3	E	E	E	E	E	E	E	E	E
	λ_{\max}		2	2	2	3	E	E	E	E	E	E	E	E	E
Dialdehyde	ϵ_{\max}	1	E	E	4	E	E	E	E	E	E	E	E	E	E
	λ_{\max}	1	E	E	4	E	E	E	E	E	E	E	E	E	E
Ketoaldehyde	ϵ_{\max}		5	6	E	E	E	E	E	E	E	E	E	E	E
	λ_{\max}		5	6	E	E	E	E	E	E	E	E	E	E	E
Diketone	ϵ_{\max}			5	E	E	E	E	E	E	E	E	E	E	E
	λ_{\max}			5	E	7	E	E	E	E	E	E	E	E	E
Hydroxyketone	ϵ_{\max}		8	E	E	E	E	E	E	E	E	E	E	E	E
	λ_{\max}		8	9	E	E	E	E	E	E	E	E	E	E	E
Acidaldehyde	ϵ_{\max}	E	E	E	E	E	E	E	E	E	E	E	E	E	E
	λ_{\max}	E	E	E	E	E	E	E	E	E	E	E	E	E	E
Hydroxyaldehyde	ϵ_{\max}	E	E	E	E	E	E	E	E	E	E	E	E	E	E
	λ_{\max}	10	E	E	E	E	E	E	E	E	E	E	E	E	E
Ketoacid	ϵ_{\max}		1	E	1	E	E	E	E	E	E	E	E	E	E
	λ_{\max}		1	E	1	E	E	E	E	E	E	E	E	E	E

Table S3: Corresponding gas and aqueous phase references for Table 1 in manuscript.

	Gaseous Reference	Aqueous Reference
Acetone	(Horowitz et al., 2001)	(Xu et al., 1993)
Levulinic acid	-	(Mackinney and Temmer, 1948)
2-oxopropanal	(Chen et al., 2000)	(Schutze and Herrmann, 2004)

3-oxobutanal	(Vavilova et al., 1981)	(Martinez et al., 1975)
2,3-butanedione	(Horowitz et al., 2001)	(Schutze and Herrmann, 2004)
Pyruvic acid	(Horowitz et al., 2001)	(Mackinney and Temmer, 1948)
Glyceraldehyde	-	This work

Computational Analysis of Additional Atmospherically Relevant Compounds

We chose four additional compounds to study that were identified in d-limonene (Fang et al., 2012) and isoprene (Jaoui et al., 2006) SOA. The computational methods and results are detailed in the text. Table S4 contains the calculated ϵ_{\max} and λ_{\max} values. With these calculated values and structure activity relationships to describe hydration equilibrium, aqueous OH rate constants, and Henry's Law constants, we determined the branching ratios Q and Z. These branching ratios are presented graphically in Figure S11.

Table S4: Calculated ϵ_{\max} and λ_{\max} values for compounds found in d-limonene and Isoprene SOA. Both 3,6-oxoheptanoic acid and ketolimonaldehyde have two peaks on their calculated spectra.

	Reference	ϵ_{\max} [$M^{-1} cm^{-1}$]	λ_{\max} [nm]
4-hydroxy-3-methyl-but-2-enal	(Fang et al., 2012)	276	493.4
3,6-oxoheptanoic acid	(Jaoui et al., 2006)	277/304	221.3/8.9
ketolimonaldehyde	(Jaoui et al., 2006)	280/299	166.6/161.2
ketonorlimonic acid	(Jaoui et al., 2006)	275	99.2

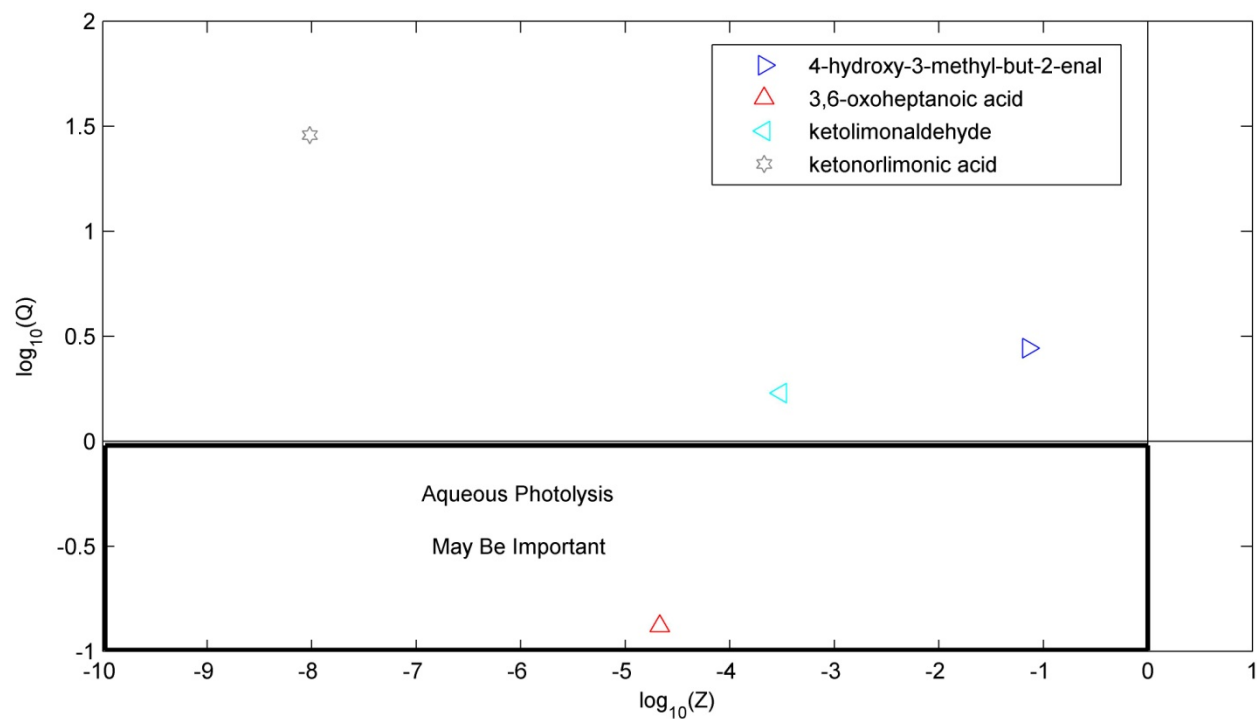


Figure S11: Q and Z analysis of compounds presented in Table S4. Aqueous hydroxyl radical concentration is 10^{-13} M, $T = 25^{\circ}\text{C}$, $\text{SZA} = 20^{\circ}$, and $\text{LWC} = 0.5 \text{ g m}^{-3}$.

Molecular Dynamics Simulation Molar Extinction Plots

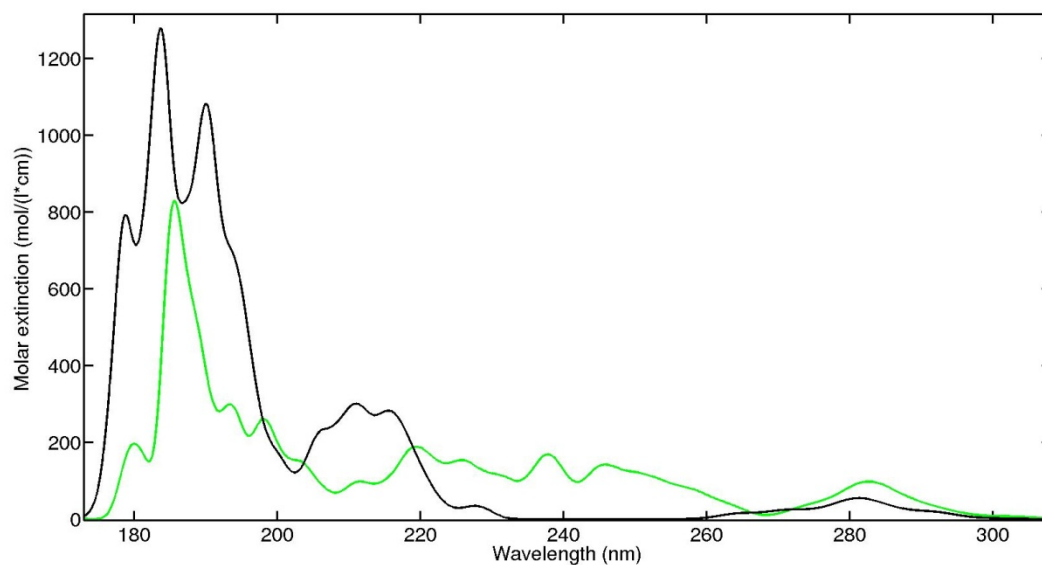


Figure S12: Calculated MD extinction coefficients for gaseous (green) and aqueous (black) levulinic acid.

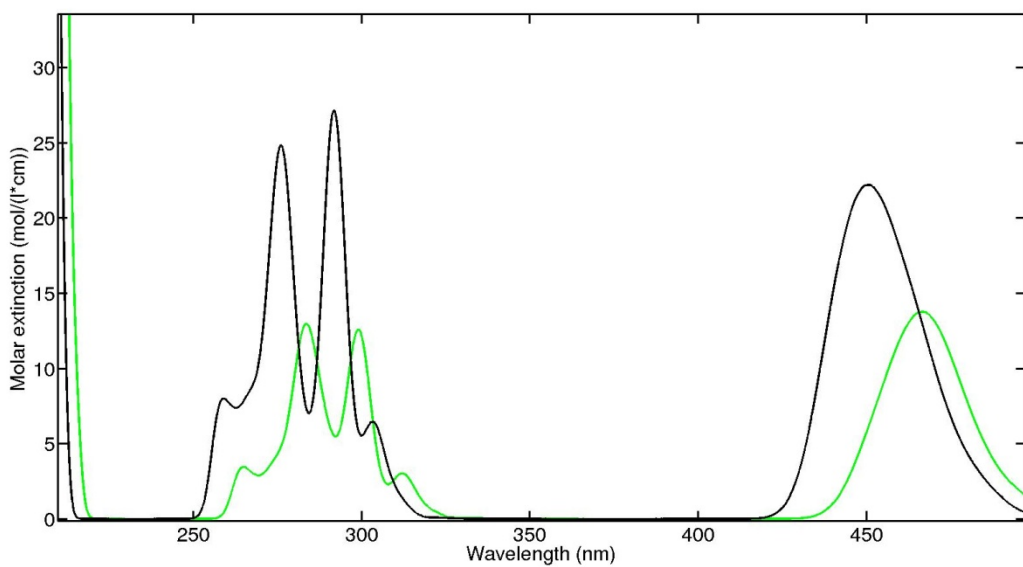


Figure S13: Calculated MD extinction coefficients for gaseous (green) and aqueous (black) 2-oxopropanal.

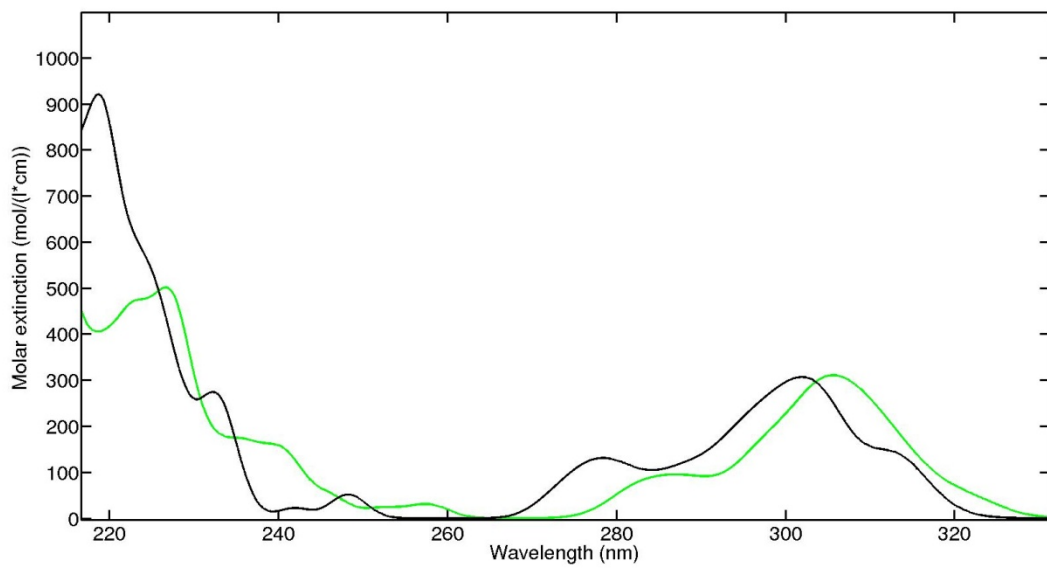


Figure S14: Calculated MD extinction coefficients for gaseous (green) and aqueous (black) 3-oxobutanal.

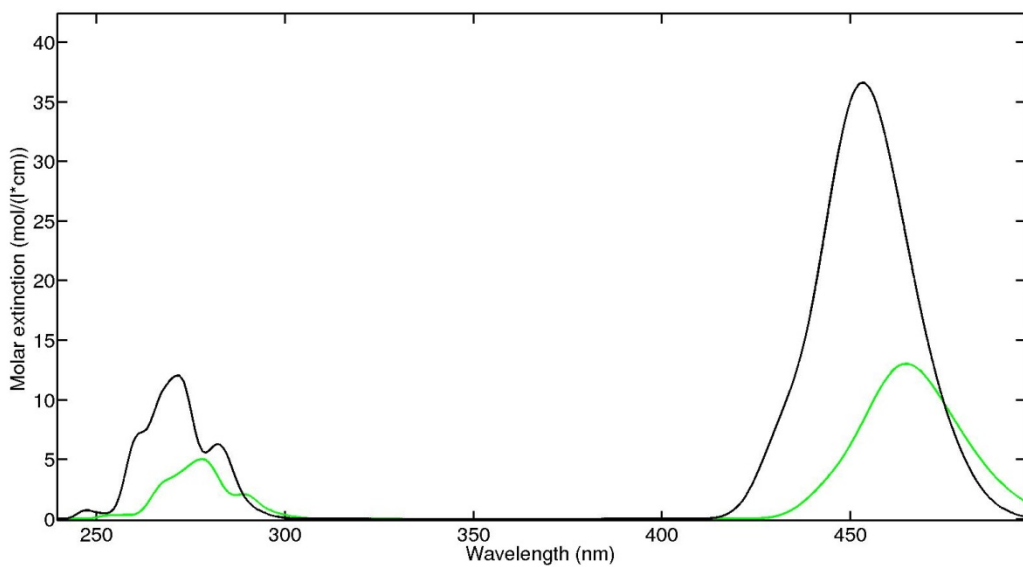


Figure S15: Calculated MD extinction coefficients for gaseous (green) and aqueous (black) 2,3-butanedione.

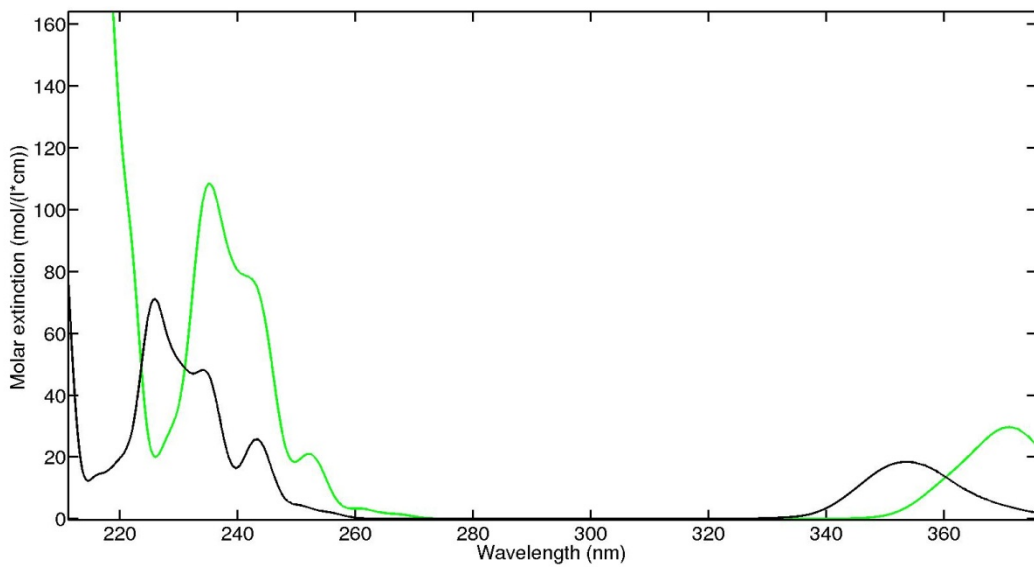


Figure S16: Calculated MD extinction coefficients for gaseous (green) and aqueous (black) pyruvic acid.

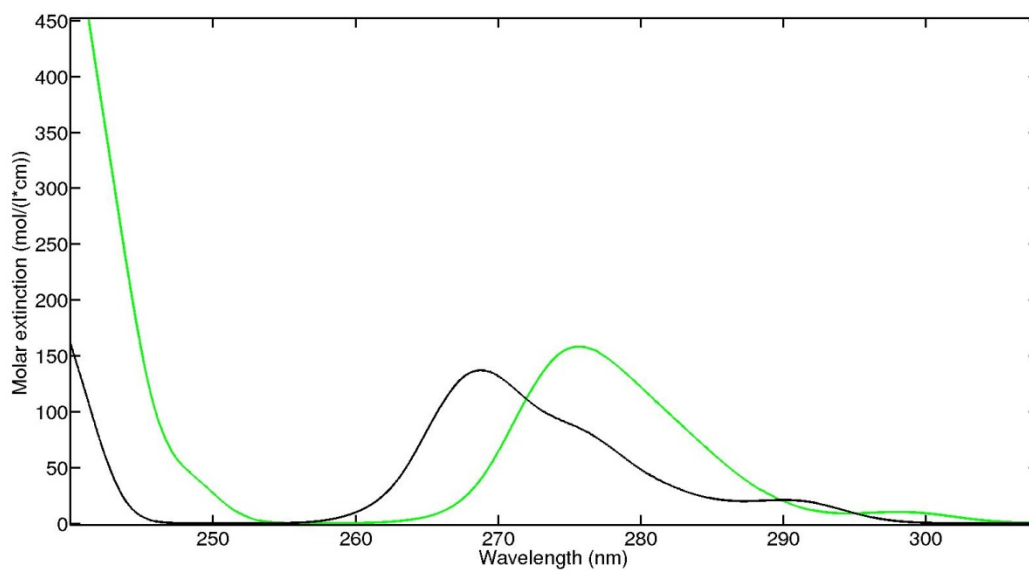


Figure S17: Calculated MD extinction coefficients for gaseous (green) and aqueous (black) glyceraldehyde.

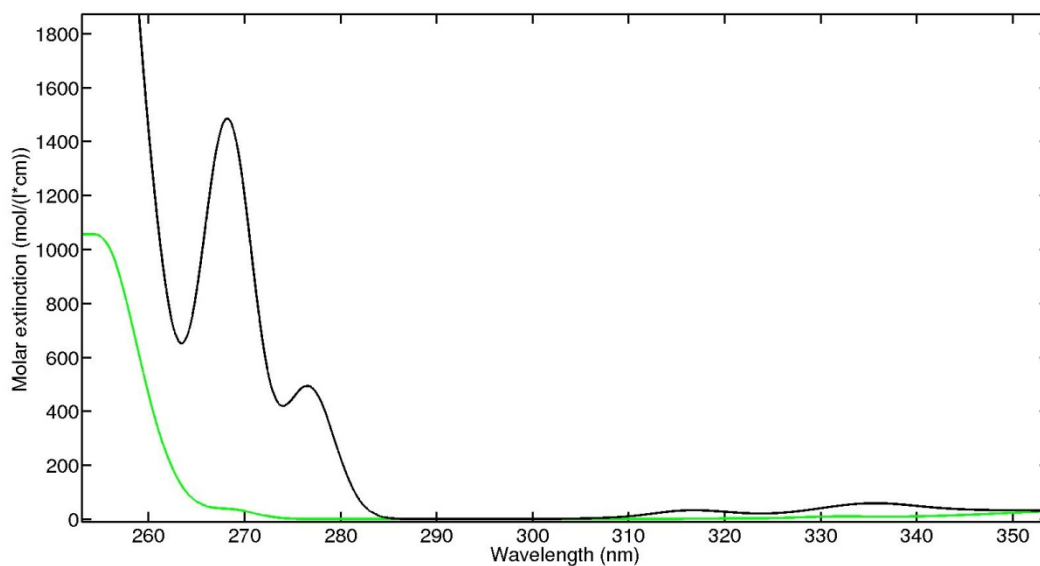


Figure S18: Calculated MD extinction coefficients for gaseous (green) and aqueous (black) 4-hydroxy-3-methyl-but-2-enal.

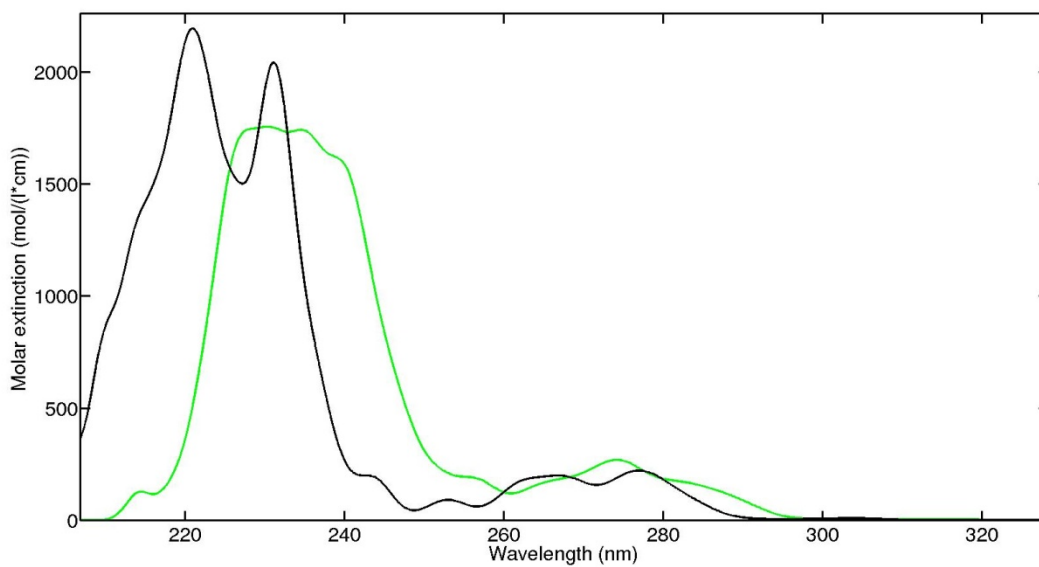


Figure S19: Calculated MD extinction coefficients for gaseous (green) and aqueous (black) 3,6-oxoheptanoic acid.

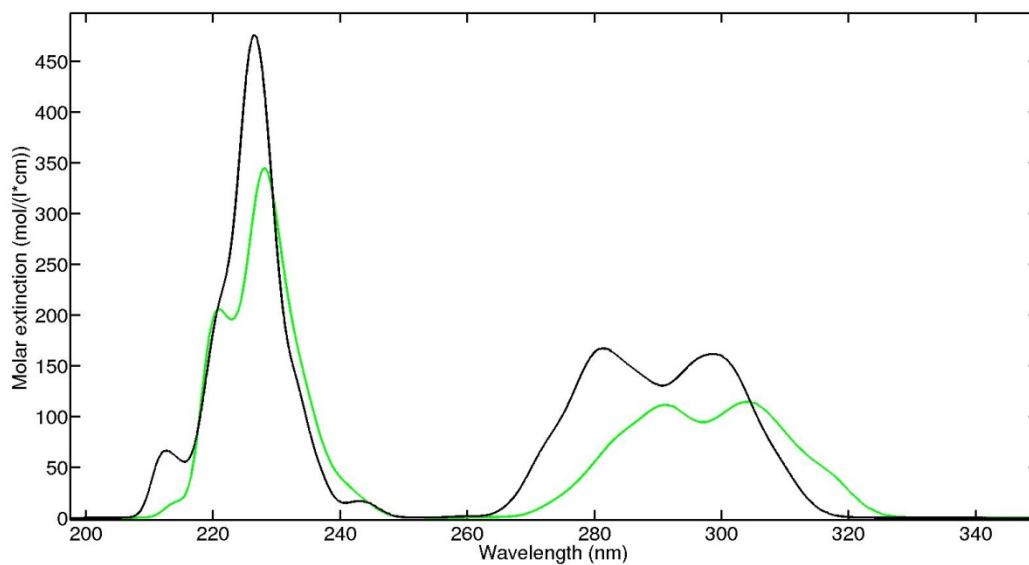


Figure S20: Calculated MD extinction coefficients for gaseous (green) and aqueous (black) ketolimonaldehyde.

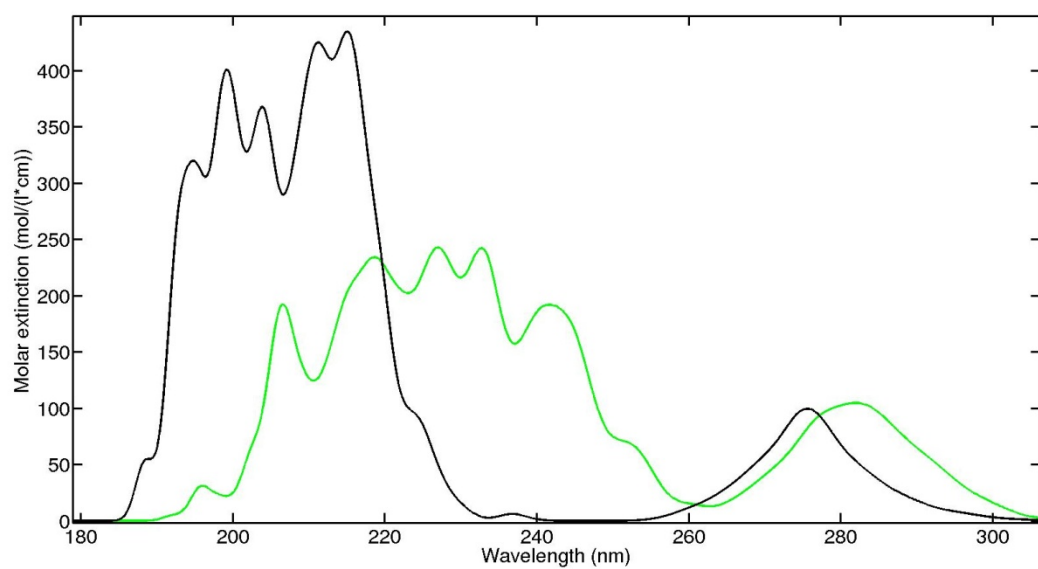


Figure S21: Calculated MD extinction coefficients for gaseous (green) and aqueous (black) ketonorlimonic acid.

Table S5: Measured extinction coefficients of glyceraldehyde.

wavelength (nm)	Extinction (1/M/cm)	uncertainty in Extinction (1/M/cm)	wavelength (nm)	Extinction (1/M/cm)	uncertainty in Extinction (1/M/cm)
200	20.5293	0.3411	241	3.0844	0.0194
201	18.9451	0.3111	242	3.0795	0.0209
202	17.5113	0.2771	243	3.0793	0.02
203	16.1821	0.2493	244	3.0817	0.018
204	14.9455	0.2283	245	3.0833	0.0163
205	13.8589	0.2152	246	3.0835	0.0168
206	12.8193	0.2115	247	3.0872	0.0199
207	11.9172	0.1989	248	3.095	0.0214
208	11.1012	0.1883	249	3.0991	0.0165
209	10.3966	0.1858	250	3.101	0.0177
210	9.6865	0.1778	251	3.1095	0.0182
211	9.0736	0.1657	252	3.1242	0.018
212	8.5425	0.1607	253	3.1395	0.0149
213	8.0363	0.1514	254	3.1559	0.0157
214	7.5723	0.138	255	3.1759	0.0183
215	7.1373	0.1286	256	3.2046	0.0202
216	6.7141	0.1178	257	3.2306	0.0197
217	6.3445	0.1108	258	3.2667	0.0174
218	5.9844	0.099	259	3.2995	0.0208
219	5.6735	0.0885	260	3.3387	0.022
220	5.362	0.0807	261	3.3784	0.0221
221	5.0918	0.069	262	3.4246	0.0183
222	4.8429	0.0638	263	3.4622	0.0208
223	4.5937	0.0578	264	3.5017	0.0255
224	4.3593	0.0556	265	3.5404	0.0234
225	4.124	0.0468	266	3.5799	0.0217
226	3.9148	0.042	267	3.6102	0.021
227	3.7195	0.0394	268	3.6364	0.0218
228	3.5613	0.0368	269	3.6539	0.0226
229	3.4356	0.0368	270	3.6702	0.0238
230	3.3332	0.0307	271	3.6779	0.0234
231	3.2658	0.0271	272	3.674	0.0256
232	3.2119	0.0252	273	3.6639	0.0251
233	3.169	0.027	274	3.6456	0.0252
234	3.1451	0.0265	275	3.6237	0.0237
235	3.128	0.0192	276	3.5929	0.0219
236	3.111	0.0182	277	3.5499	0.0246
237	3.099	0.0197	278	3.5038	0.0251
238	3.0933	0.0211	279	3.4563	0.0227
239	3.0907	0.0202	280	3.399	0.0246
240	3.0839	0.0196	281	3.3337	0.0224

Table S5: Measured extinction coefficients of glyceraldehyde (continued).

wavelength (nm)	Extinction (1/M/cm)	uncertainty in Extinction (1/M/cm)	wavelength (nm)	Extinction (1/M/cm)	uncertainty in Extinction (1/M/cm)
282	3.2647	0.0235	324	0.626	0.0013
283	3.1949	0.02	325	0.5962	0.0006
284	3.1189	0.0211	326	0.5725	0.0043
285	3.0384	0.021	327	0.5518	0.001
286	2.9552	0.0211	328	0.5196	0.0018
287	2.8765	0.0184	329	0.5004	0.0007
288	2.7898	0.0154	330	0.4828	0.0032
289	2.6972	0.0162	331	0.4637	0.0031
290	2.6077	0.015	332	0.4416	0.0049
291	2.5178	0.0138	333	0.4237	0.004
292	2.427	0.0127	334	0.4127	0.0033
293	2.3341	0.0121	335	0.3956	0.0046
294	2.2435	0.0122	336	0.3779	0.0047
295	2.1552	0.0127	337	0.3607	0.002
296	2.069	0.0115	338	0.354	0.0005
297	1.985	0.0076	339	0.3442	0.005
298	1.8987	0.0086	340	0.3303	0.0037
299	1.818	0.0086	341	0.3176	0.0007
300	1.7436	0.0076	342	0.3083	0.0011
301	1.672	0.0075	343	0.2995	0.0015
302	1.6004	0.0088	344	0.2917	0.0048
303	1.5307	0.007	345	0.2809	0.0046
304	1.4643	0.0073	346	0.2737	0.0022
305	1.3988	0.004	347	0.2724	0.004
306	1.3331	0.006	348	0.2615	0.0033
307	1.2729	0.0028	349	0.2553	0.0023
308	1.2204	0.0027	350	0.2498	0.0049
309	1.1729	0.0047	351	0.2449	0.0011
310	1.1175	0.0036	352	0.2423	0.0026
311	1.0706	0.0039	353	0.2357	0.005
312	1.033	0.0027	354	0.2252	0.0023
313	0.9915	0.0058	355	0.217	0.0012
314	0.9504	0.004	356	0.2203	0.0042
315	0.9122	0.0022	357	0.2183	0.005
316	0.8732	0.0022	358	0.209	0.0017
317	0.8367	0.0021	359	0.2083	0.0011
318	0.8037	0.0026	360	0.2035	0.0027
319	0.7693	0.0034	361	0.201	0.0006
320	0.7359	0.0021	362	0.197	0.0033
321	0.7073	0.0037	363	0.1949	0.0061
322	0.68	0.0032	364	0.192	0.0057
323	0.6517	0.0049	365	0.1867	0.004

Table S5: Measured extinction coefficients of glyceraldehyde (continued).

wavelength (nm)	Extinction (1/M/cm)	uncertainty in Extinction (1/M/cm)
366	0.1812	0.0047
367	0.1751	0.0031
368	0.1747	0.0025
369	0.1705	0.0063
370	0.1671	0.0054
371	0.1585	0.0006
372	0.1631	0.0017
373	0.1613	0.0045
374	0.155	0.0049
375	0.1522	0.0025
376	0.1539	0.0023
377	0.1475	0.0023
378	0.1434	0.0059
379	0.1414	0.0033
380	0.1408	0.0012
381	0.136	0.0019
382	0.1344	0.0018
383	0.1303	0.0035
384	0.1247	0.0023
385	0.1215	0.002
386	0.1244	0.0031
387	0.1212	0.0026
388	0.115	0.0008
389	0.116	0.0005
390	0.1149	0.0001
391	0.1086	0.0034
392	0.1073	0.0041
393	0.1061	0.0027
394	0.1055	0.0014
395	0.1018	0.0033
396	0.1	0.0041
397	0.0986	0.0016
398	0.0984	0.001
399	0.0942	0.003
400	0.0917	0.0031

Table S6: Measured extinction coefficients of dihydroxyacetone.

wavelength (nm)	Extinction (1/M/cm)	uncertainty in Extinction (1/M/cm)	wavelength (nm)	Extinction (1/M/cm)	uncertainty in Extinction (1/M/cm)
200	6.3218	0.1996	284	13.5282	0.027
202	8.0359	1.1151	286	12.3095	0.027
204	13.4457	4.1652	288	11.1104	0.0416
206	21.1199	6.4318	290	9.813	0.0416
208	27.1587	4.0366	292	8.5274	0.0566
210	25.4327	0.74	294	7.2693	0.0204
212	18.3718	0.1419	296	6.0977	0.0367
214	12.3684	0.0705	298	5.0559	0.0416
216	8.0595	0.0914	300	4.1045	0.0255
218	5.2407	0.0638	302	3.2789	0.0136
220	3.5029	0.0367	304	2.6066	0.0189
222	2.5004	0.0255	306	1.9382	0.0068
224	1.9815	0.0255	308	1.4664	0.0068
226	1.8124	0.0104	310	1.0733	0.0068
228	1.8753	0.0189	312	0.8099	0.0136
230	2.1387	0.0136	314	0.5779	0.0068
232	2.5161	0	316	0.4207	0.0068
234	2.9801	0.0111	318	0.3027	0.0189
236	3.5541	0.0136	320	0.2241	0.0068
238	4.2578	0.0189	322	0.1691	0.0068
240	5.0755	0.0104	324	0.1179	0
242	5.9994	0.0255	326	0.0904	0.0068
244	6.9469	0.0358	328	0.0708	0.0167
246	7.9966	0.0056	330	0.055	0.0056
248	9.0699	0.0189	332	0.0275	0.0068
250	10.1943	0.0189	334	0.0432	0.0104
252	11.3423	0.0233	336	0.0236	0.0056
254	12.4549	0.0272	338	0.0315	0.0111
256	13.5754	0.0068	340	0	0
258	14.5897	0.0322	342	0.0157	0.0056
260	15.5058	0.0377	344	0.0039	0.0104
262	16.3196	0.0367	346	0.0275	0.0068
264	17.0036	0.034	348	0.0118	0.0068
266	17.5423	0.0111	350	0.0118	0.0068
268	17.8135	0.0204	352	0.0157	0.0056
270	17.9472	0.0152	354	0.0157	0.0056
272	17.8293	0.0233	356	0.0118	0.0068
274	17.5619	0.0312	358	0.0236	0.0056
276	17.1177	0.0516	360	0.0197	0.0152
278	16.4296	0.0367	362	0	0
280	15.5765	0.0389	364	0.0157	0.0136
282	14.633	0.0409	366	0	0.0068

Table S6: Measured extinction coefficients of dihydroxyacetone (continued)

wavelength (nm)	Extinction (1/M/cm)	uncertainty in Extinction (1/M/cm)
368	0.0157	0.0056
370	0	0
372	0.0118	0.0068
374	0	0
376	0	0
378	0	0
380	0	0
382	0.0118	0.0068
384	0	0.0124
386	0	0
388	0	0
390	0	0
392	0	0
394	0	0
396	0	0
398	0	0
400	0	0

References

Beeby, A., Mohammed, D. b. H., and Sodeau, J. R.: Photochemistry and photophysics of glycolaldehyde in solution, *J. Am. Chem. Soc.*, 109, 857-861, 10.1021/ja00237a036, 1987.

Chen, Y., Wang, W., and Zhu, L.: Wavelength-dependent photolysis of methylglyoxal in the 290-440 nm region, *J. Phys. Chem. A*, 104, 11126-11131, 10.1021/jp002262t, 2000.

Davis, L.: The structure of dihydroxyacetone in solution, *Bioorg. Chem.*, 2, 197-201, 1973.

Fang, W., Gong, L., Zhang, Q., Cao, M., Li, Y., and Sheng, L.: Measurements of secondary organic aerosol formed from oh-initiated photo-oxidation of isoprene using online photoionization aerosol mass spectrometry, *Environ. Sci. Tech.*, 46, 3898-3904, 10.1021/es204669d, 2012.

Glushonok, G. K., Petryaev, E. P., Turetskaya, E. A., and Shadyro, O. I.: Equilibrium between the molecular forms of glycolaldehyde and of dl-glyceraldehyde in aqueous solutions, *Zh. Fiz. Khim.*, 60, 2960-2970, 1986.

Glushonok, G. K., Glushonok, T. G., Maslovskaya, L. A., and Shadyro, O. I.: A ¹h and ¹³c nmr and uv study of the state of hydroxyacetone in aqueous solutions, *Russ. J. Gen. Chem.*, 73, 1027-1031, 10.1023/b:rugc.0000007604.91106.60, 2003.

Gubina, T. I., Pankratov, A. N., Labunskaya, V. I., and Rogacheva, S. M.: Self-oscillating reaction in the furan series, *Chem. Heterocycl. Compd.*, 40, 1396-1401, 10.1007/s10593-005-0051-5, 2004.

Horowitz, A., Meller, R., and Moortgat, G. K.: The uv-vis absorption cross sections of the alpha-dicarbonyl compounds: Pyruvic acid, biacetyl and glyoxal, *J. Photochem. Photobiol.*, A, 146, 19-27, 10.1016/S1010-6030(01)00601-3, 2001.

Jaoui, M., Corse, E., Kleindienst, T. E., Offenberg, J. H., Lewandowski, M., and Edney, E. O.: Analysis of secondary organic aerosol compounds from the photooxidation of d-limonene in the presence of nox and their detection in ambient pm2.5, *Environ. Sci. Tech.*, 40, 3819-3828, 10.1021/es052566z, 2006.

Mackinney, G., and Temmer, O.: The deterioration of dried fruit. Iv. Spectrophotometric and polarographic studies, *J. Am. Chem. Soc.*, 70, 3586-3590, 10.1021/ja01191a013, 1948.

Malik, M., and Joens, J. A.: Temperature dependent near-uv molar absorptivities of glyoxal and gluteraldehyde in aqueous solution, *Spectrochim. Acta, Part A*, 56, 2653-2658, 2000.

Maroni: *Annales de Chimie*, 13, 757-787, 1957.

Martinez, A. M., Cushmac, G. E., and Rocek, J.: Chromic acid oxidation of cyclopropanols, *J. Am. Chem. Soc.*, 97, 6502-6510, 10.1021/ja00855a036, 1975.

Rice, F. O.: The effect of solvent on the ultra violet absorption spectrum of a pure substance, *J. Am. Chem. Soc.*, 42, 727-735, 10.1021/ja01449a009, 1920.

Schutze, M., and Herrmann, H.: Uptake of acetone, 2-butanone, 2,3-butanedione and 2-oxopropanal on a water surface, *PCCP*, 6, 965-971, 2004.

Steenken, S., Jaenicke-Zauner, W., and Schulte-Frohlinde, D.: Photofragmentation of hydroxyacetone, 1,3-dihydroxyacetone, and 1,3-dicarboxyacetone in aqueous solution. An epr study, *Photochem. Photobiol.*, 21, 21-26, 10.1111/j.1751-1097.1975.tb06624.x, 1975.

Vavilova, A. N., Trofimov, B. A., and Volkov, A. N. K., V. V. : *Journal of Organic Chemistry USSR (English Translation)*, 17, 809-812, 1981.

Xu, H., Wentworth, P. J., Howell, N. W., and Joens, J. A.: Temperature dependent near-uv molar absorptivities of aliphatic aldehydes and ketones in aqueous solution, *Spectrochim. Acta, Part A*, 49, 1171-1178, 1993.